



## ESTIMATION OF TIME-RESOLVED 3D PRESSURE FIELDS IN AN IMPINGING JET FLOW FROM DENSE LAGRANGIAN PARTICLE TRACKING

F. Huhn, A. Schröder<sup>c</sup>, D. Schanz, S. Gesemann, P. Manovski<sup>2</sup>

German Aerospace Center (DLR), Institute of Aerodynamics and Flow Technology, Göttingen, Germany

<sup>2</sup> DSTG, Aerodynamics & Aeroelasticity, Aerospace Division, Melbourne, Australia

<sup>c</sup>Corresponding author: Tel.: +495517092190; Email: andreas.schroeder@dlr.de

### KEYWORDS:

**Main subjects:** Unsteady 3D pressure, dense accelerometry, data assimilation, flow visualization

**Fluid:** turbulent impinging jet flow

**Visualization method(s):** 3D Lagrangian particle tracking with Shake-The-Box, FlowFit

**Other keywords:**

**ABSTRACT:** *Lagrangian particle tracking (LPT) using the Shake-The-Box (STB) method enables a dense and accurate 3D measurement of position, velocity and acceleration vectors of a large amount of single seeding tracers imaged by a multiple camera system. A subsequent application of the data assimilation technique “FlowFit” to the reconstructed particle tracks provides access to the full time resolved velocity gradient tensor together with the 3D pressure (gradient) fields. A perpendicular impinging jet flow with exit velocities at  $U = 1, 4$  and  $16$  m/s and nozzle to plate spacing of  $H/D = 5$  has been investigated using large-volume STB. Helium-filled soap bubbles are used as tracer particles which are illuminated with pulsed LED arrays. A large measurement volume has been covered (cloud of tracked particles in a volume of 54 liters,  $\sim 190,000$  particles). The reconstructed time-resolved 3D pressure fields have been validated against microphone recordings at the wall with high correlation coefficients up to  $R = 0.88$ . In this paper the experimental conditions are described together with the main processing parameters adopted for the STB strategy and the applied FlowFit data assimilation method. Results are shown in terms of instantaneous flow and pressure fields together with comparisons to time-traces of synchronously measured microphone signals.*

### 1 Introduction

The measurement of the pressure field in aerodynamic and turbulent flows is of high interest, for example, for the estimation of unsteady fluid dynamic loads and forces on structures to study aero-elastic problems, for the determination of sources of aero-acoustic noise, and for the computation of the pressure-diffusion term in the transport equation of turbulent kinetic energy. Pressure transducers and microphones can be used to obtain a local point-wise measurement of pressure. They are often mounted in walls, and also free-field pressure probes exist. However, unlike the intrusive measurement with sensors, the pressure field is also indirectly accessible through an optical nonintrusive flow measurement of fields of the material acceleration. The pressure gradient and the material acceleration are the dominant terms in the momentum equation (1) and therefore directly linked by this equation. van Oudheusden [23] reviews the development of pressure reconstruction from flow measurements that dates back to the year 1935 and made significant progress in the last two decades, mainly based on velocity data gained from particle image velocimetry (PIV) [11].

Recent examples of studies dealing with pressure reconstruction from flow measurements include a comparison of stereoscopic and tomographic (tomo) PIV in the wake of a square cylinder [2], tomo PIV measurements in a turbulent boundary layer [4] [10] [18], time-resolved tomoPIV around an airfoil [7], a scanning tomo PIV experiment around a flapping wing [21], a tomo PIV measurement with

subsequent particle tracking in the wake of a wall-mounted cylinder [17], cf. [8] [19]. Most of the studies validate their results against other pressure measurements or against theoretical predictions. Except for the last two, the listed studies are based on time-resolved PIV data and consequently obtain the material acceleration from the Eulerian velocity field by computing the low-pass filtered material derivative indirectly. A very recent comparison of a broad scope of techniques for pressure reconstruction [22] shows, however, that the accuracy of the pressure field determination can be considerably improved with dense Lagrangian particle tracking (LPT) where the material acceleration is directly obtained from individual particle trajectories. Nowadays, with the *Shake-The-Box (STB)* Lagrangian particle tracking technique [13] [15] time-resolved series of particle images with densities of  $\sim 0.1$  ppp and above can be processed accurately which allow to simultaneously track up to 300,000 particles for typical 4 Mpx high-speed cameras [5] [16]. Furthermore, a new four-pulse STB technique is available, which allows the required determination of velocity and acceleration fields by Lagrangian particle tracking as well in high-speed flows [9]. In their most recent review article on the development of load estimation techniques [12] explicitly propose that the STB technique will become the new standard for instantaneous pressure reconstruction and state its importance for future measurements of unsteady flows.

In our experimental investigation time-resolved volumetric pressure fields have been reconstructed in a perpendicular impinging jet flow with exit velocities at  $U = 1, 4$  and  $16$  m/s and a nozzle-plate spacing of  $H/D = 5$  from Lagrangian particle tracking with high seeding concentration. The Shake-The-Box method [15] has been employed for dense particle tracking and subsequently the FlowFit data assimilation technique [3] has been applied to the particle track data in order to gain 3D velocity and pressure fields. Helium-filled soap bubbles (HFSB) are used as tracer particles [1] which are illuminated by high-power pulsed LED arrays at  $1.25$  kHz acquisition rate. A large measurement volume of  $54$  liters has been covered enabling particle tracking of up to  $\sim 190,000$  particles simultaneously. The reconstructed time-resolved 3D pressure fields have been validated against local flush mounted microphone recordings at the wall with high correlation coefficients up to  $R = 0.88$ . In a reduced measurement volume ( $13$  liters) it was demonstrated that dense Lagrangian particle tracking is feasible up to the maximal possible jet velocity of  $U = 16$  m/s. This fact indicates the possibility to apply large-volume flow measurements by STB using HFSB as well in low-speed wind tunnels, in which the interference-free introduction of the HFSB tracers in a sufficient number and density is one major challenge (see e.g. ISFV 18 contribution of Schanz et al.). Further details of the present experimental investigation can be found in [6].

The experimental set-up, acquisition strategy of particle images, STB evaluation method and post-processing steps using FlowFit for gaining continuous 3D velocity and pressure field reconstructions are described in section 2, while the gained time-resolved volumetric pressure and flow field results are presented in section 3 together with comparisons of sampled 3D pressure signals at the wall with time-series of pressure fluctuations measured by three flush mounted microphones.

## 2 Method

In the present study, we combine three new techniques in the field of particle based measurement methods, Shake-The-Box Lagrangian particle tracking (LPT), helium-filled soap bubbles (HFSB) and use of high-power LEDs for pulsed volumetric illumination of the bubbles in order to measure the flow of an impinging jet. The impinging jet was chosen as a generic flow with substantial pressure fluctuations that has many practical applications. An air jet generated by an 8-bladed fan with stators (PHYWE - 02742-93) and a nozzle exit diameter of  $0.11$  m impinges on a flat acrylic glass plate at an angle of  $\theta = 90^\circ$ . The flow is seeded with HFSBs with a diameter of  $300$ - $500$   $\mu\text{m}$  depending on the air

pressure supplied to the generator (LaVision HFSB generator, 10 nozzles). For a single measurement run, the flow chamber was seeded in advance for a time  $> 5$  min and the seeding generator was left running during the measurement. The HFSBs are illuminated by three over-pulsed high-power LED arrays, including two arrays of 42 LEDs each (HARDsoft Microprocessor Systems) operated at 90 A (voltage 44 V). The illuminated cross-sectional area has a size of  $\sim 200$  mm in depth and  $\sim 450$  mm in radial direction along the glass plate. All LED arrays are equipped with collimating lenses on top of each single LED and are operated at 10% duty cycle. A mirror plate below the fan is used to increase the illumination by back reflection.

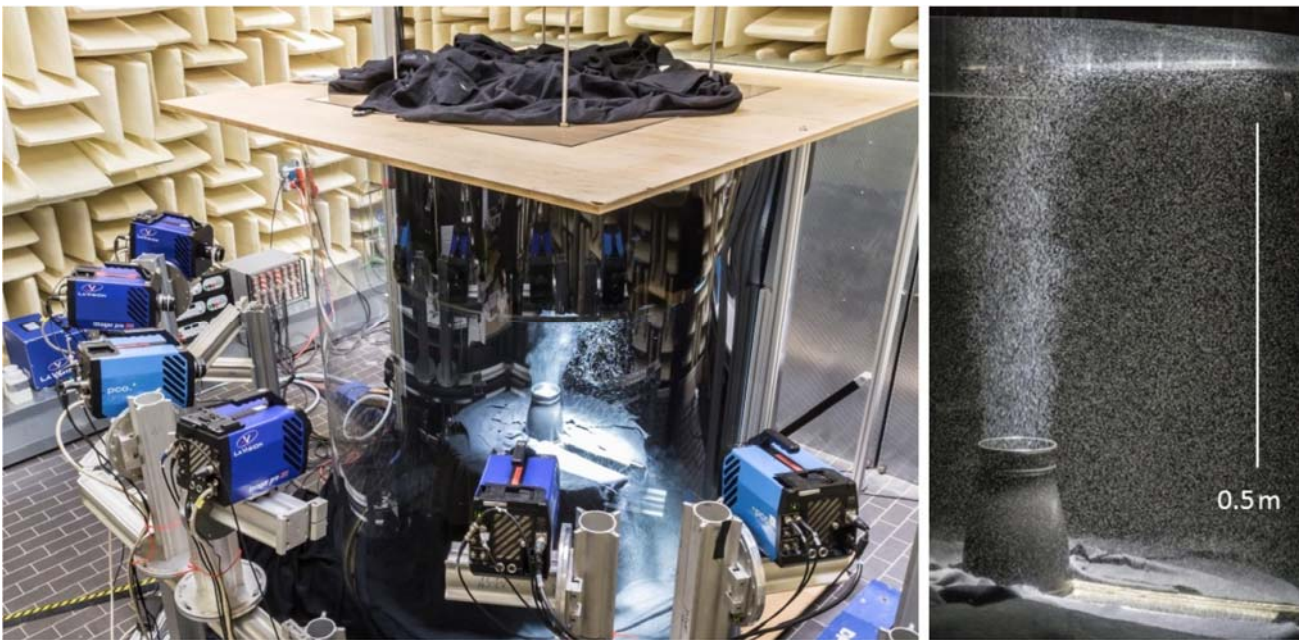


**Fig. 1: Experimental setup. (a) Camera setup and flow chamber. (b) Jet nozzle and impinging jet seeded with HFSB tracers. At the top, the locations of the three microphones in the impingement plate appear as bright dots.**

The measurement volume, extending from the wall to the fan nozzle exit (530 mm in streamwise direction) is imaged by six high-speed cameras (PCO dimax S4 and LaVision Imager pro HS 4M). The cameras are positioned in an in-line configuration and oriented in a way that those lines-of-sight imaging the wall surface are tangential to the flat plate. For the calibration of the cameras, a large 2D calibration target ( $77 \times 95$  cm<sup>2</sup>, black dots, diameter 10 mm, spacing 45 mm) on a translation stage is aligned with the centerline of the jet and is translated -100 mm and +100 mm in z-direction. Volume self-calibration (VSC) [24] is used to refine the camera calibration. The experimental setup is shown in Fig.1.

The STB evaluation [15] technique has been adapted to the series of particle images from all 6 camera projections, which requires the calibration of the particles optical transfer function (OTF) for each camera and sub-volume [14] and a proper parametrization of the iterative 3D particle reconstruction scheme (IPR) [25] for the initialization phase of STB and the 3D particle position correction (“shaking”) after each prediction step. Particle tracks with discrete positions are then fit with a continuous function consisting of cubic B-splines (TrackFit, [3]) The coefficient for the smoothing term in the cost function is based on the cross-over frequency of the particle position frequency

spectrum and is chosen such that particle tracks are low-pass filtered with a cut-off frequency of  $0.3f_{Ny}$ , with the Nyquist frequency  $f_{Ny}$ . Velocity and acceleration are obtained as the temporal derivatives of the continuous B-spline function. With a model for the position frequency spectrum, the uncertainties of position, velocity and acceleration of the fitted trajectories can be estimated as  $\varepsilon_x = 16 \mu\text{m}$  ( $\sim 0.05$  pixels),  $\varepsilon_v = 0.01 \text{ m/s}$  and  $\varepsilon_a = 14 \text{ m/s}^2$  for the  $U = 4 \text{ m/s}$  flow case. In general, STB Lagrangian particle tracking with high seeding densities is well suited for the measurement of mean fields in the flow. Bin averaging of velocity and acceleration, that are accurately measured based on single trajectories with subpixel accuracy, yields mean fields [20]. Due to the large number of particles, a high spatial resolution (small bins down to  $\sim 0.1 \text{ px}$ ) of the mean fields and a small uncertainty (many particles per bin) can be reached with reasonable experimental effort. Due to the high position accuracy, the mean acceleration field can be obtained close to walls, such that mean wall pressure fields on aerodynamic models are obtained by a simple integration of the mean acceleration field.

In a next step instantaneous pressure fields are reconstructed from velocity and acceleration data along the tracks with the interpolation and data assimilation scheme FlowFit [3]. In the FlowFit approach both measured fields, velocity  $\mathbf{u}$  and acceleration  $\mathbf{a}$ , and the full momentum equation

$$\frac{D\mathbf{u}}{Dt} = -\nabla\bar{p} + \nu\Delta\mathbf{u} = \frac{\partial\mathbf{u}}{\partial t} + (\mathbf{u} \cdot \nabla)\mathbf{u} \quad (1)$$

coupling both measured quantities are considered for the pressure reconstruction.

The two fields  $\mathbf{u}$  and  $P$  are used as fit variables. Acceleration is expressed in terms of  $\mathbf{u}$  and  $P$  by Eq. (1). The velocity field is regularized by  $\nabla \cdot \mathbf{u} = 0$ . Combining the further condition  $\nabla \cdot \frac{\partial\mathbf{u}}{\partial t} = 0$ , with the material derivative and the momentum equation leads to the condition  $\Delta\bar{p} = \nabla \cdot (\mathbf{u} \cdot \nabla)\mathbf{u}$  for the two fit variables. This last condition is quadratic in  $\mathbf{u}$  and leads to a non-linear optimization problem which is solved with a Limited-memory Broyden-Fletcher-Goldfarb-Shanno (L-BFGS) solver (see [3]). At the wall we impose symmetric boundary conditions, i.e., the measured flow quantities  $\mathbf{u}$  and  $\mathbf{a}$  are mirrored at the wall, i.e., about the  $x$ - $z$  plane. These boundary conditions correspond to setting the normal vector components of velocity and acceleration to zero at the wall,  $\mathbf{u}_{y|w} = 0$  and  $\mathbf{a}_{y|w} = 0$ , where the  $w$ -subscript denotes the evaluation at the wall. For the simpler momentum Eq. (1) this translates to the condition  $\frac{\partial P}{\partial y}|_w = 0$ . This is in line with the observation that in a turbulent boundary layer the pressure at a small distance to the wall is a good estimate for the wall pressure itself [10]. Applying the above estimated uncertainties values found for particle velocity and acceleration to the calculation of the error of the pressure reconstruction for a corresponding wavenumber window between two times the mean particle distance,  $\lambda_2 = 12 \text{ mm}$  and a typical domain size,  $\lambda_1 = 200 \text{ mm}$ , i.e.,  $[k_1, k_2] = [31, 524] \text{ rad/m}$  the uncertainty of the pressure field remains in the order of  $\sigma_N \sim 0.1 \text{ Pa}$  (details in [6]). This uncertainty seems rather small and would correspond to a dynamic pressure range of  $\sim 60:1$ . However, it is a rough estimate and additional error sources may exist. On one hand, aliasing due to undersampling of small flow structures possibly leads to an additional error that is excluded in the above value.

The interpolated pressure and velocity fields are represented as a dense grid of cubic B-splines with a step width of  $\Delta x = 3 \text{ mm}$ , half the mean particle distance of  $6 \text{ mm}$ , corresponding to a particle density of  $0.125$  particles per B-spline cell [ppc]. The B-spline coefficients are found by a fit to the scattered data. The cost functions include terms for spatial smoothing and for a regularization of the solution with additional physical constraints from the Navier-Stokes-equation. The present wall allows for the

installation of microphones for a validation of the pressure reconstruction. Three condenser microphones (G.R.A.S. 40BF 1/4", diameter of diaphragm 5.9 mm) are flush mounted in the impinging plate at distances of  $1D$ ,  $2D$  and  $3D$  from the jet center. The frequency response is flat ( $\pm 2$  dB) in the range from 4 Hz to 100 kHz. Microphone data is recorded with a 16-bit VIPER- 48 (gbm) multi-channel acquisition system at a frequency of 250 kHz, high-pass filtered with a 1.5 Hz cut-off frequency. Microphone recordings are synchronized with the flow measurement by recording the trigger (enable) signal of the LED illumination on an additional channel. Noise from the fan and its motor is the main source of uncertainties of the microphone pressure signal. However, in the relevant frequency range of 5–150 Hz, the signal to noise ratio has been measured to be in the order of  $10^4$ , i.e., the amplitude error of the microphone pressure signal is  $\sim 1\%$  and therefore negligible w.r.t. the accuracy discussed here.

The study has two objectives, first, we show the applicability of LPT with LED illuminated HFBSs in a large volume for higher flow velocities than in previous experiments [5], and second, we validate the reconstructed pressure field. We achieve a measurement volume of 54 liters for a jet velocity of  $U = 1$  and 4 m/s and a rectangular volume of 13 liters at  $U = 16$  m/s with a reduced field-of-view due to frame rate limitations. To the best knowledge of the authors, the reconstructed volumetric pressure field with a volume of 30 liters is the largest reported so far (cf. [12] [17] [23]).

### 3 Results

The velocity fields of the impinging jet is presented for the slowest and fastest measured jet velocity,  $U = 1$  m/s and  $U = 16$  m/s. The slow case is recorded at a frame rate of 1.25 kHz with an LED pulse width of 100  $\mu$ s. For the fast case, both parameters are adjusted to a frame rate of 3.9 kHz with an LED pulse width of 27  $\mu$ s, in order to avoid streaking of the particle images and to reliably track also the fastest and most accelerated particles. To reach the high recording frequency, the camera resolution has to be reduced to 576 x 1728 pixels. Approximately 190,000 particles can be tracked simultaneously for the slow case in a volume of 54 liters, and 40,000 for the fast case in a volume of 13 liters. An example of the reconstructed particle tracks is shown in Fig. 2.

An example of a reconstructed 3D pressure field together with the Q-value for visualization of vortical motions is presented in Fig. 3. For this case at  $U = 1$  m/s, extended spatial and temporal coherent vortical structures can be resolved in the shear layer and in the wall jet region. The rectangular box in Fig. 3 marks the region of negligible flow which is used as a reference for the absolute pressure and thus as a value for the pressure off-set correction. In a first step the mean pressure over the box is set to be zero at each time step by subtracting the spatial mean value over the box from the entire pressure field.

For the reconstruction of the pressure field, we focus on the experimental results with a jet velocity of  $U = 4$  m/s recorded at 1 kHz. For this velocity, we can expect more pronounced pressure fluctuations than for the slower velocity of  $U = 1$  m/s, while the appearing flow structures can be better resolved spatially and temporally with the installed measurement equipment than in the extreme case at  $U = 16$  m/s. In the shear layer at the nozzle radius of the jet ( $x/D = 0.5$ ), strong pressure fluctuations develop due to strong vortices which are advected upwards and impact on the wall at  $x/D \sim 0.5$  leading to large pressure fluctuations at the position of microphone 1 (black dot). The corresponding reconstructed pressure fields in a x-y-plane (showing the mirror-wall boundary condition) and at the wall in a x-z-plane are shown in Fig. 4. Here, further outwards, following the flow in radial direction, the chain of

alternating high and low pressure regions continues along the wall adjacent to microphone 2 and 3. The stagnation region with high pressure (maximum fluctuations reaching  $\sim 12$  Pa) is a distinct feature in the pressure field.

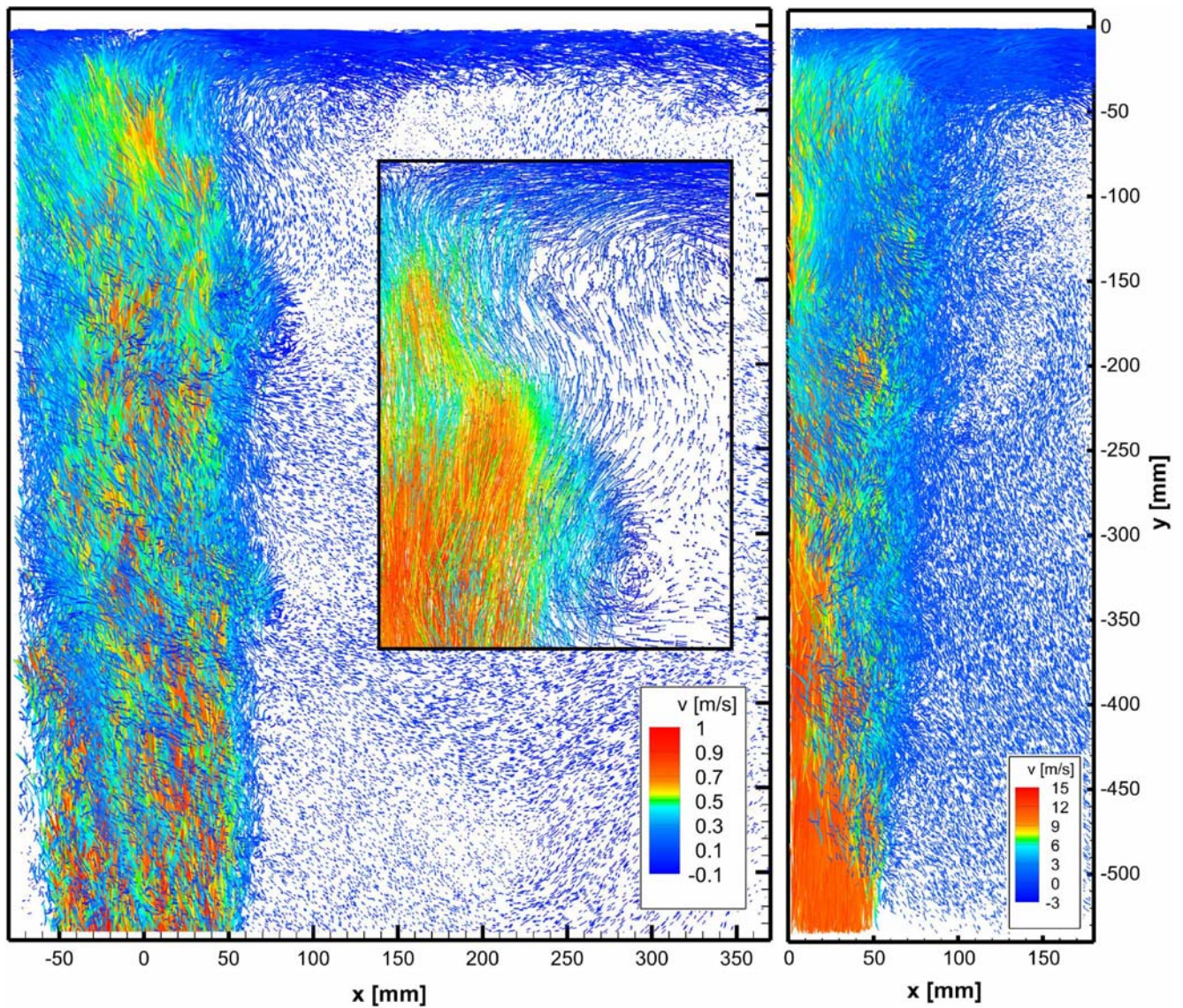


Figure 1. Lagrangian particle tracks reconstructed by Shake-The-Box displayed using nine successive time-steps, color-coded by y-velocity for two jet velocities (Left:  $U = 1$  m/s , Right:  $U = 16$  m/s)

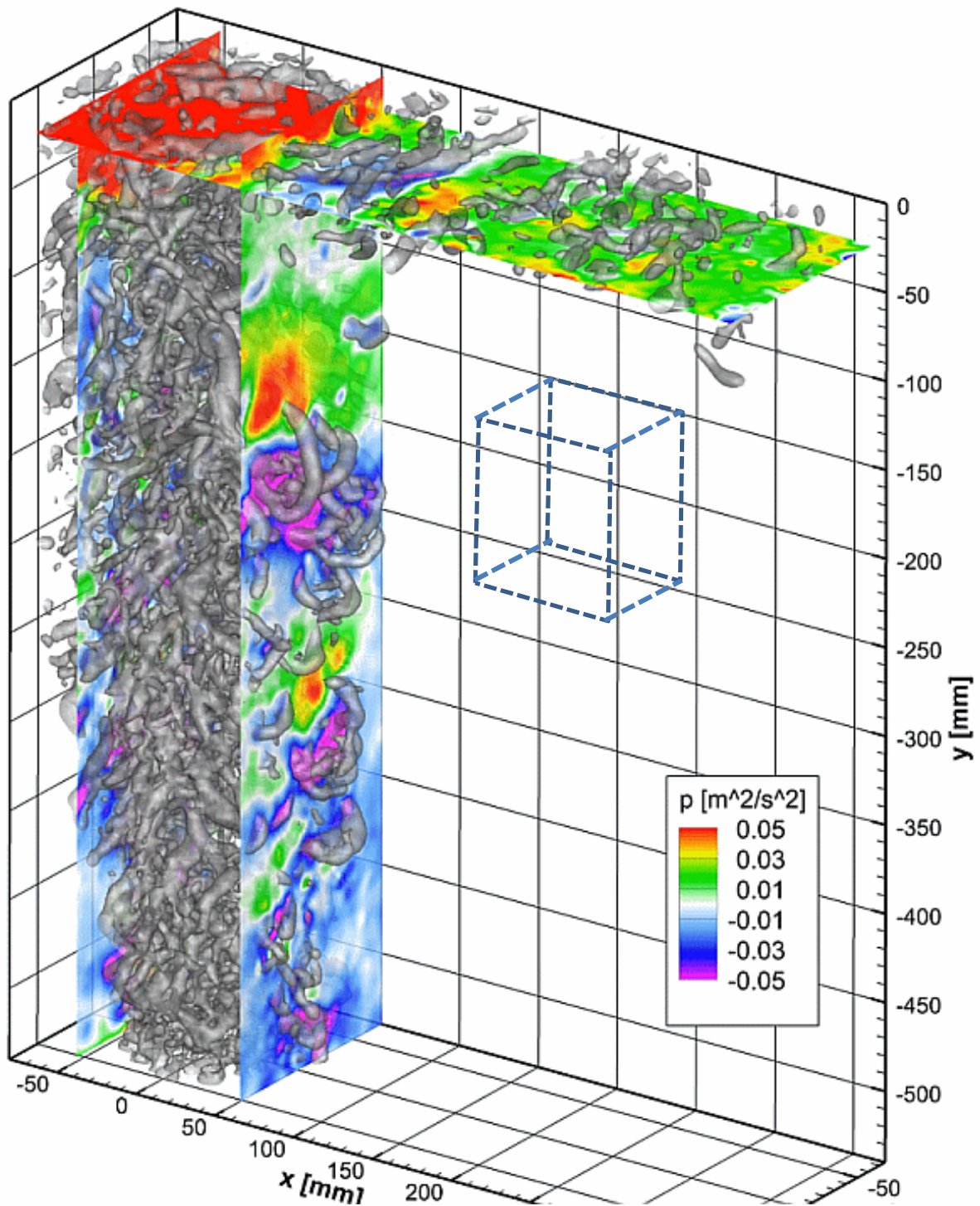
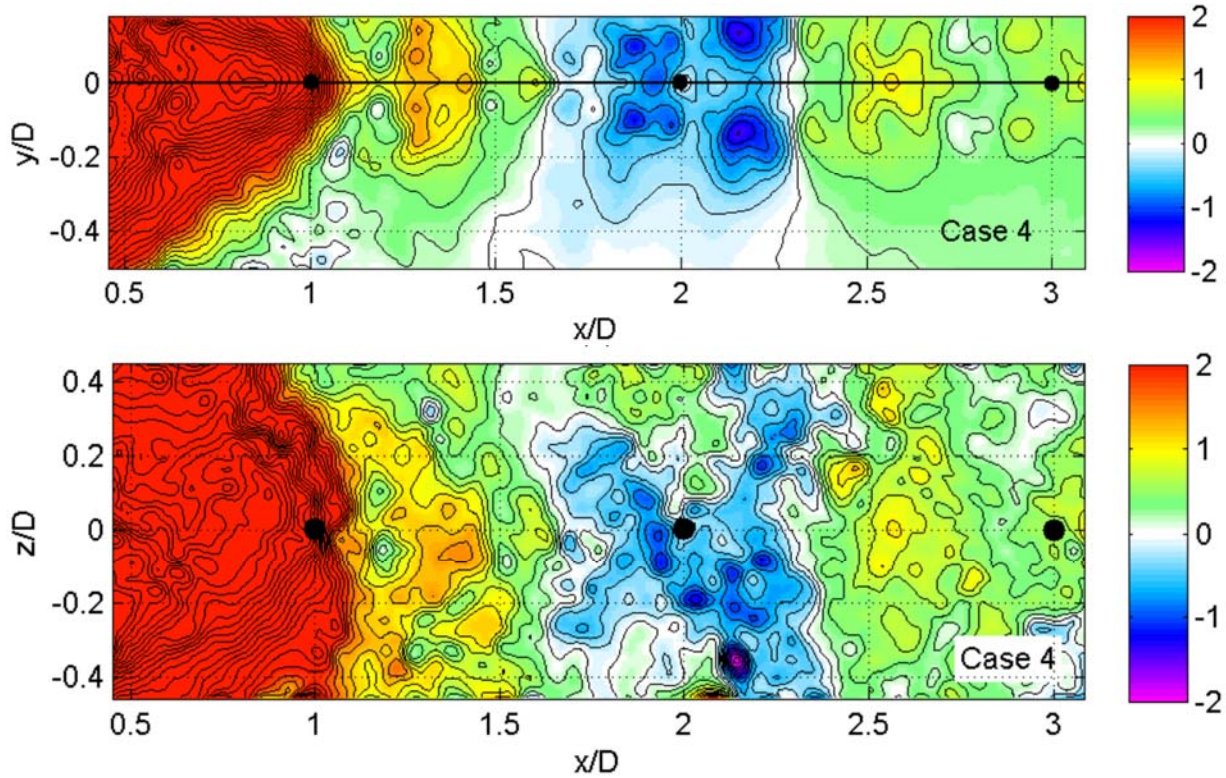


Figure 2. 3D pressure field reconstruction from STB and FlowFit. Snapshot from a time-resolved series of impinging jet flow with iso-contour surfaces of Q-value for visualization of vortical motions.



**Figure 3. Lateral central slice (x-y-plane) (top) and at the wall (x-z-plane) (bottom) of the reconstructed pressure field  $P(x)$  [Pa] at  $U = 4$  m/s using full non-linear FlowFit data assimilation and symmetric (“mirrored”) boundary conditions at the wall. The wall is drawn as a black line (top), dots represent three microphone positions. Range of contour lines [-6; 6] Pa with increment 0.2 Pa.**

The comparison of the two pressure time series in Fig. 5 visualizes the agreement between microphone pressure and LPT pressure in a direct way. The pressure offset (black curve) is a small value and can be ruled out as a reason for the discrepancy between both signals. We obtain a high correlation coefficient of  $R = 0.88$  for microphone 1. This value is among the highest reported in literature for pressure reconstruction from a turbulent boundary layer flow measurement. To some extent, the uncertainty of the reconstructed pressure field can be quantified based on the difference between both pressure data sets in Fig. 5. The standard deviation of the difference signal is 0.36 Pa, 0.30 Pa, and 0.26 Pa, for microphone 1, 2 and 3. Assuming that the microphone recording has a negligible uncertainty, the magnitude of the difference signal can be interpreted as an uncertainty of the pressure field. This uncertainty of  $\sim 0.3$  Pa is clearly higher than the value of  $\sim 0.1$  Pa derived above from the uncertainty of the acceleration data. It seems that some uncertainty is added during the step of pressure reconstruction with FlowFit. To validate the reconstruction strategy against the microphone measurements, we compute the Pearson correlation coefficient  $R = \langle P_1(t)P_2(t) \rangle / (\sigma_1\sigma_2)$  for the two time series, the pressure estimation from flow measurement  $P_1(t)$  and the pressure recorded from the microphones  $P_2(t)$  with their standard deviations  $\sigma_1$  and  $\sigma_2$ . Both pressure time series have first been filtered using a Butterworth filter with bandpass range [3,150] Hz, the lower limit removing small frequencies and the upper limit corresponding to the low-pass cutoff frequency of the LPT trajectories when fit with a B-spline curve (TrackFit) [3]. Then, the microphone data have been downsampled to the LPT frequency by linear interpolation. The high correlation coefficients  $\langle R \rangle = 0.77$ ;  $R_{\max} = 0.88$

between the reconstructed pressure field and the microphone pressure signals show that the dominant pressure fluctuations of the flow can be reliably obtained from the LPT flow measurement even in such large volumes.

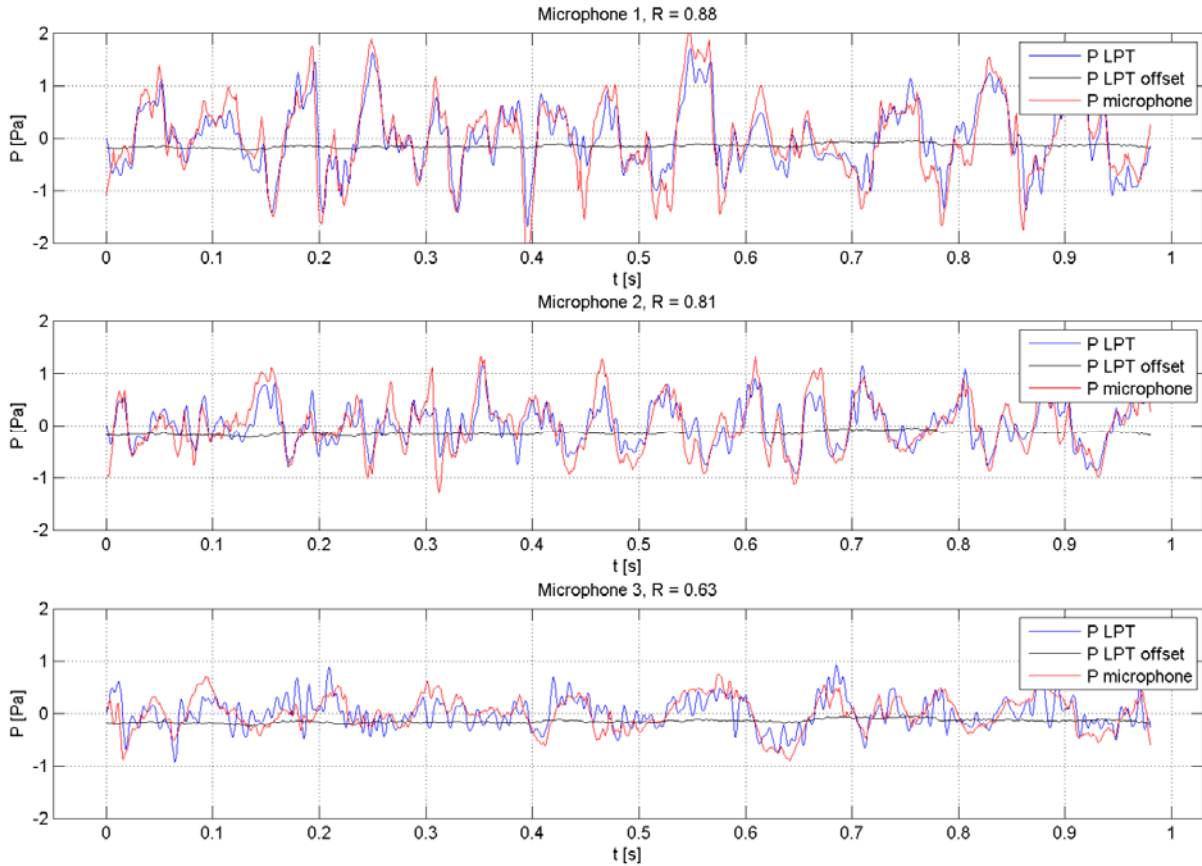


**Figure 4. Direct comparison of pressure time series of the three microphones (red) and the reconstructed pressure from LPT (blue) at  $U = 4$  m/s. The pressure offset is shown in black. Data is shown for the reconstruction with FlowFit. Both pressure time series are bandpass filtered in the range [3; 150] Hz.**

## 4 Conclusions

In the presented measurement, we are able to reconstruct the time-resolved 3D pressure field in a larger volume compared to previous pressure reconstructions [4] [10] [17] using HFSBs, LED illumination, high-speed cameras and Lagrangian particle tracking. A local validation of the reconstructed pressure at critical points in the wall boundary layer shows that the dominant pressure fluctuations of the impinging jet (10 - 20 Hz) are well captured by the flow measurement. Smaller pressure fluctuations with higher temporal and spatial frequencies are less resolved at the chosen spatial and temporal resolution of the measurement; however, they are also less relevant for the estimation of loads on the wall. The good agreement of the LPT pressure and the microphone pressure used as reference can be attributed to the accurate determination of the particle acceleration with STB, which has been shown to give better results than correlation based flow measurement techniques [22], and the Navier-Stokes-constraint data assimilation approach FlowFit. The uncertainty of the measured acceleration is directly

dependent on the position accuracy of tracked particles, which itself relies on the clear imaging of single particles. Using HFSB as large tracer particles has been shown to be suitable to image large measurement volumes [5] [17]. Temporal and spatial resolution of the measurement limits the spectral range of pressure fluctuations that can be reconstructed. More details of the present study can be found in [6].

In conclusion, the use of highly seeded Lagrangian particle tracking with the Shake-The-Box [15] approach allows for the measurement of velocity and acceleration fields and the reconstruction of the time-resolved 3D pressure fields by FlowFit down to the wall of structures or models in a large volume. In low speed flows, unsteady pressure fluctuations in the order of  $\sim 0.5$  Pa can be reliably measured. With this sensitivity, the method extends the accessible measurement range to small instantaneous pressure fluctuations that cannot be detected with pressure sensitive paint (PSP). Pressure reconstruction from dense Lagrangian particle tracking offers the possibility to derive small forces and moments on wings and models in the wind tunnel. It is therefore ideal for the study of unsteady flow phenomena and the induced loads on structures, e.g., for efficiency studies in biomimetic propulsion or for the localization of the sources of aero-acoustic noise close to walls.

## Acknowledgements

The authors would like to thank Janos Agocs, Stefan Haxter, Thomas Ahlefeldt, Dirk Michaelis, Uwe Dierksheide and Jiggar Shah for their help during the setup and execution of the experiment. We acknowledge the support of LaVision GmbH with camera equipment and the seeding generator. Work including the experimental results has partly been funded by the DFG-project *Analyse turbulenter Grenzschichten mit Druckgradient bei großen Reynoldszahlen mit hochauflösenden Vielkammermessverfahren* (grant KA 1808/14-1 and SCHR 1165/3-1).

## References

- [1] Bosbach J, Kühn M, Wagner C (2009) Large scale particle image velocimetry with helium filled soap bubbles. *Exp Fluids* 46:539–547
- [2] de Kat R, van Oudheusden BW (2012) Instantaneous planar pressure determination from PIV in turbulent flow. *Exp Fluids* 52:1089–1106
- [3] Gesemann S, Huhn F, Schanz D and Schröder A. From Noisy Particle Tracks to Velocity, Acceleration and Pressure Fields using B-splines and Penalties. *18th Int Symp on the Application of Laser Techniques to Fluid Mechanics*, July 4-7, Lisbon, Portugal, 2016.
- [4] Ghaemi S, Ragni D, Scarano F (2012) PIV-Based pressure fluctuations in the turbulent boundary layer. *Exp Fluids* 53:1832–1840
- [5] Huhn F, Schanz D, Gesemann S, Dierksheide U, van de Meerendonk R, Schröder A (2017) Large-scale volumetric flow measurement in a pure thermal plume by dense tracking of helium-filled soap bubbles. *Exp Fluids* 58:116
- [6] Huhn F, Schanz D, Manovski P, Gesemann S, Schröder A (2018), Time-resolved large-scale volumetric pressure fields of an impinging jet from dense Lagrangian particle tracking. *Exp Fluids* 59:81
- [7] Jeon YJ, Earl T, Braud P, Chatellier L, David L (2015) 3D pressure field around an inclined airfoil by tomographic TR-PIV and its comparison with direct pressure measurements, 18th Int. Symp. on Applications of Laser Techniques to Fluid Mechanics, Lisbon, Portugal

- [8] Novara M, Scarano F (2013) A particle-tracking approach for accurate material derivative measurements with tomographic PIV. *Exp Fluids* 54:1584
- [9] Novara M, Schanz D, Reuther N, Kähler CJ and Schröder A. Lagrangian 3D particle tracking in high-speed flows: Shake-The-Box for multi-pulse systems. *Exp in Fluids*, 57:128, 2016.
- [10] Pröbsting S, Scarano F, Bernardini M, Pirozolli S (2013) On the estimation of wall pressure coherence using time-resolved tomographic PIV. *Exp Fluids* 54:1567
- [11] Raffel M, Willert CE, Scarano F, Kähler CJ, Wereley ST, Kompenhans J (2018) Particle image velocimetry: a practical guide, 3<sup>rd</sup> edition, Springer
- [12] Rival D, van Oudheusden BW (2017) Load-estimation techniques for unsteady incompressible flows. *Exp Fluids* 58:20
- [13] Schanz D, Schröder A, Gesemann S, Michaelis D, Wieneke B (2013) Shake-the-Box: a highly efficient and accurate Tomographic Particle Tracking Velocimetry (TOMO-PTV) method using prediction of particle position, 10th Int. Symposium on Particle Image Velocimetry—PIV13 (Delft, The Netherlands, July 1-3)
- [14] Schanz D, Gesemann S, Schröder A, Wieneke B, Novara M (2013) Non-uniform optical transfer functions in particle imaging: calibration and application to tomographic reconstruction. *Meas Sci Technol* 24:024009
- [15] Schanz D, Schröder A, Gesemann S (2016) Shake-The-Box: Lagrangian particle tracking at high particle image densities. *Exp Fluids* 57:70
- [16] Schanz D, Huhn F, Gesemann S, Dierksheide U, van de Meerendonk R, Manovski P, Schröder A (2016) Towards high-resolution 3D flow field measurements at cubic meter scales, 18th Int. Symp. on Applications of Laser Techniques to Fluid Mechanics, Lisbon, Portugal
- [17] Schneiders JFG, Caridi GCA, Sciacchitano A, Scarano F (2016) Large-scale volumetric pressure from tomographic PTV with HFSB tracers. *Exp Fluids* 57:164
- [18] Schneiders JFG, Pröbsting S, Dwight RP, van Oudheusden BW, Scarano F (2016) Pressure estimation from single-snapshot tomographic PIV in a turbulent boundary layer. *Exp Fluids* 57:53
- [19] Schröder A, Geisler R, Staack K, Elsinga GE, Scarano F, Wieneke B, Henning A, Poelma C, Westerweel J (2011) Eulerian and Lagrangian views of a turbulent boundary layer flow using time-resolved tomographic PIV. *Exp Fluids* 50:1071–1091
- [20] Schröder A, Schanz D, Michaelis D, Cierpka C, Scharnowski S and Kähler CJ (2015) “Advances of PIV and 4D-PTV ”Shake-The-Box” for Turbulent Flow Analysis – the Flow over Periodic Hills”, *Flow Turbulence and Combustion*, 95 (2-3): 193-209
- [21] Tronchin T, David L, Farcy A (2015) Loads and pressure evaluation of the flow around a flapping wing from instantaneous 3D velocity measurements. *Exp Fluids* 56:7
- [22] van Gent PL, Michaelis D, van Oudheusden BW, Weiss PE, de Kat R, Laskari A, Jeon YJ, David L, Schanz D, Huhn F, Gesemann S, Novara M, McPhaden C, Neeteson NJ, Rival DE, Schneiders JFG and Schrijer FFJ. (2017) Comparative assessment of pressure field reconstructions from particle image velocimetry measurements and Lagrangian particle tracking. *Exp Fluids*, 58:33.
- [23] Van Oudheusden BW (2013). PIV-based pressure measurement. *Meas Sci Technol*, 24 032001.
- [24] Wieneke B (2008) Volume self-calibration for 3D particle image velocimetry. *Exp Fluids* 45:549–556
- [25] Wieneke B. (2013) Iterative reconstruction of volumetric particle distribution. *Meas Sci Technol*, 24 024008.